



AALBORG UNIVERSITY

STUDENT REPORT

ED5-3-E16

Hovering control of a quadcopter

Students:

Alexandra Dorina Török
Andrius Kulšinskas

Supervisors:

Christian Mai

December 5, 2016



AALBORG UNIVERSITY

STUDENT REPORT

School of Information and
Communication Technology
Niels Bohrs Vej 8
DK-6700 Esbjerg
<http://sict.aau.dk>

Title:
Hovering control of a quadcopter

Abstract:

xxx

Theme:
Scientific Theme

Project Period:
Autumn Semester 2016

Project Group:
ED5-3-E16

Participant(s):
Alexandra Dorina Török
Andrius Kulšinskas

Supervisor(s):
Christian Mai

Copies: x

Page Numbers: 41

Date of Completion:
December 5, 2016

The content of this report is freely available, but publication (with reference) may only be pursued due to agreement with the author.

Contents

Preface	1
1 Introduction	2
1.1 Introduction	2
2 General characteristics of a quadcopter	4
2.1 Systems of coordinates	4
2.2 Working principle	5
2.3 Quadcopter manouvering	6
2.4 Assumptions	8
3 Physical setup	9
4 Quadcopter Model	12
4.1 Quaternions and Euler angles	12
4.2 BLDC Motor	14
4.3 Quadcopter Dynamics	18
4.4 Kinematics	18
4.5 Motor Dynamics	19
4.6 Forces	20
4.7 Torques	21
4.8 Equations of Motion	22
4.9 Control	22

5 Sensors	24
5.1 Model of the sensors	24
5.1.1 Programming Accelerometer and Gyroscope	24
6 Actuators	26
6.1 Propeller model	26
6.2 Motor model	26
6.2.1 Expected and Real Motor Performance	26
6.2.2 APM Output and Motor Speed Relationship	28
6.3 Electronic Speed Controllers	32
6.3.1 Calibrating and Programming ESCs	32
7 State space model	34
8 Experiments	35
8.0.1 Output Operating Range	35
8.0.2 APM Frequency	35
9 Discussion	38
10 Conclusion	39
Bibliography	40
11 Appendix	41
11.1 Appendix code	41

Preface

The project entitled *Hovering control of a quadcopter* was made by two students from the Electronics and Computer Engineering programme at Aalborg University Esbjerg, for the P5 project during the fifth semester.

From hereby on, every mention of 'we' refers to the two co-authors listed below.

Aalborg University, December 5, 2016.

Andrius Kulšinskas
<akulsi14@student.aau.dk>

Alexandra Dorina Török
<atarak14@student.aau.dk>

Chapter 1

Introduction

1.1 Introduction

The theme of this semester's project lies within *Automation*. Automation can be simply described as being the use of diverse control systems for fulfilling a certain task with little to no human interaction. As known from the previous semester, a control system is an instrument which has the role of adapting the behaviour of a system according to a desired state, also known as steady-state or reference. Any control system has three components: measurement, control and actuation. Without one of these, automation would not be possible. Essentially, the measure reflects the current state of the system, the controller is the brain that given the measurement decides which action will be performed and the actuator is the one executing the action.

Project ideas around the topic of automation are unlimited, since it is so widely spread. Having discussed a few of them that would meet the semester's requirements, we finally decided to work on the control of a quadcopter. Our decision was, for the most part, based on the fact that the university had the required equipment available, which enabled us to start working on the project right away.

UAVs have been attracting attention for many decades now. Powered UAVs were, at first, utilized by the military to execute reconnaissance missions. Nowadays, they have found other uses, such as aerial photography, search and rescue, delivery, geographic mapping and more. While there are different types of UAVs, our focus is on the multicopters. Multicopter can be defined as a rotorcraft with more than two motors. Based on this, the four most common types are tricopter, quadcopter, hexacopter and octocopter, each having 3, 4, 6 and 8 motors respectively. Each type of multicopter has its ups and downs - more motors mean higher liftforce and more reliable stability, but they also increase both price and damage caused in case of an error. Due to their price, size and ease of setup, quadcopters are the most popular type. They are popularly referred to as drones. Our goal for the project is to design a control system that makes it possible for the quadcopter to be stable - hovering mid-air - and to also act according to the user's input - maneuvering. Basically, our

input will be a certain height and the quadcopter will have to automatically adjust to that height and maintain its stability when no further inputs are given. A safety feature - obstacle avoidance - will also be implemented.

Chapter 2

General characteristics of a quadcopter

Before delving into the mathematical modelling of the quadcopter, it is important to understand a few basic concepts in regards to the working principles of a quadcopter and the frames in which the final model will be defined.

2.1 Systems of coordinates

Describing the movement of the quadcopter in a three dimensional space can be done by using two frames, which can be seen in Figure . The NED frame is the one that we refer to in our daily life. It points towards North, East and Downwards normal to the surface of Earth. The origin of the NED coordinate system is fixed in O. The frame can also be referred to as inertial and the vectors expressed in it will be marked with I . The other frame is fixed on the quadcopter, therefore it is called Boxy-fixed frame. It has the center in O_C , which is the center of mass of the quadcopter. Its' three axis are x,y and z. The x axis points towards one of the motors, the z axis points to the ground and the y axis completes the orthogonal coordinate system. The vectors described in this frame will be market with B .

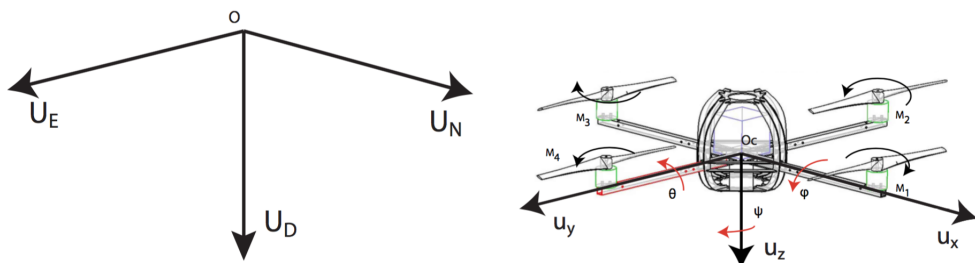


Figure 2.1: Inertial and Body-fixed frames

Besides the coordinate system, Figure also shows the hexagonal placement of the

four motors, the spinning direction of each of them and the roll - ϕ , pitch - θ and yaw - ψ angles.

The quadcopter's position represents the O to O_C displacement:

$$P^I = [X, Y, Z]^T \quad (2.1)$$

The quadcopter's velocity is express as:

$$V^B = [U, V, W]^T \quad (2.2)$$

The quadcopter's rotation can be described using the 3 Euler angles φ , θ and ψ as:

$$\Psi = [\varphi, \theta, \psi]^T \quad (2.3)$$

The quadcopter's angular velocity can be expressed using the angular velocity about the u_x axis - P, the angular velocity about the u_y axis - Q and the angular velocity about the u_z axis - R:

$$\Omega^B = [P, Q, R]^T \quad (2.4)$$

2.2 Working principle

To have an understanding of how a quadcopter actually works like, it is important to know the forces affecting it. See figure .

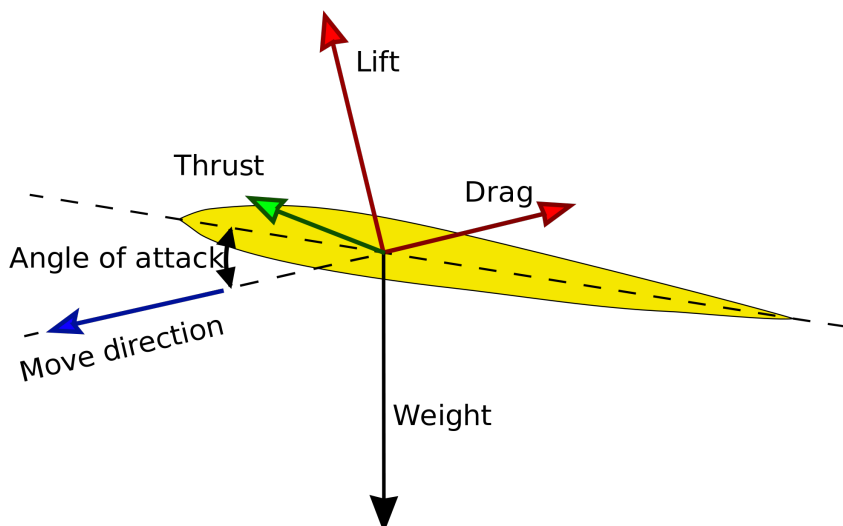


Figure 2.2: Forces affecting an aerial vehicle.

The 4 main forces acting on the quadcopter - or any aerial vehicle, for that matter are:

- **Drop** (gravitational force) affects the vehicle at all times. As any object on Earth, its mass is driven towards the centre of the planet. This force is always expressed as: $F_g = mg$, where m is the mass of the drone and g is the gravitational constant.
- **Thrust** is the force generated by the motors that is allowing the vehicle to move towards its heading. In case of a quadcopter, this force only exists when the force generated by the motors is uneven.
- **Lift** is the force created through a difference in the air pressure above and below the motor (according to Bernoulli's principle). Quadcopter's motors constantly generate lift force, which must be higher than the drop force in order for the vehicle to take flight.
- **Draw** is the resistance created by the air as the vehicle moves through it. It opposes the thrust force and therefore must be lower than the thrust force in order for the quadcopter to move on. In cases when there is no wind, such as indoors area, this force can be disregarded due to lack of wind.

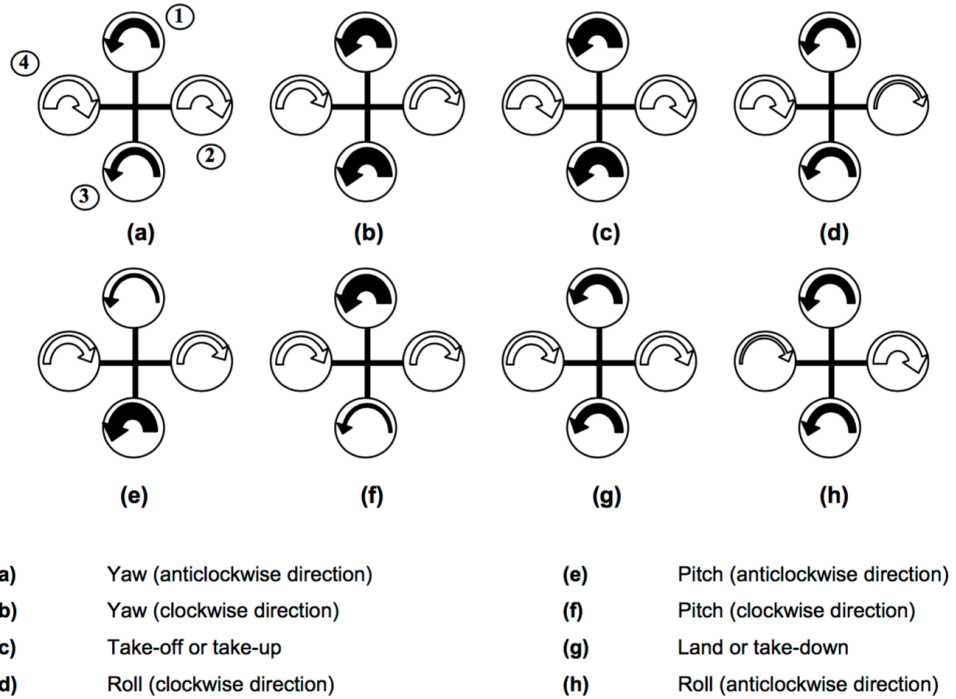
If the motors are powered off, the only force affected is the drop and therefore the quadcopter stays on the ground. In order to lift it up, we need to understand the relationship between quadcopter and thrust to weight ratio - or TWR for short. This ratio can be determined by equation F_t/F_g and describes the vehicle's ability to move up. With TWR expressed as a number, assuming that each motor generates equal amount of thrust, three cases can be identified:

- **TWR<1**: The gravitational force is higher than the lift force and therefore the quadcopter is drawn towards the ground.
- **TWR=1**: The forces are equal, causing quadcopter's altitude to stay constant.
- **TWR>1**: The thrust is higher than drop force, allowing vehicle to move upwards.

Therefore, in order to get a quadcopter up in the air, it is necessary to generate enough thrust for TWR ratio to be higher than one. In order to land it, the TWR must be smaller than 1, allowing the quadcopter to move downwards.

2.3 Quadcopter manouvering

Quadcopters are made with four identical motors, each of them having an attached propeller. As it can be seen in Figure , each pair of propellers rotate in different directions. The odd numbered motors have clockwise rotation, while even numbered motors have counter-clockwise rotation. The speed of the motors has to be adjusted in order to obtain the manouvers shown in Figure .

**Figure 2.3:** Quadcopter Rotation System.

The arrows in Figure represent the angular speeds of the motors and they can be written as:

$$\omega = [\omega_1, \omega_2, \omega_3, \omega_4]^T \quad (2.5)$$

The quadcopter's possible motions can be splitted into four categories:

- **Rolling motion** is represented by the rotation of the quadcopter about the u_x axis and it can be obtained when ω_2 and ω_4 are manipulated. In order to obtain a positive rolling, ω_4 is decreased while ω_2 is increased. The opposite will result in a negative rolling motion. Both movements can be seen in cases (a) and (b).
- **Pitch motion** is represented by the rotation of the quadcopter about the u_y axis and it can be obtained when ω_1 and ω_3 are manipulated. In order to obtain a positive pitch, ω_3 is decreased while ω_1 is increased. The opposite will result in a negative pitch motion. Both movements can be seen in cases (c) and (d).
- **Yaw motion** is represented by the rotation of the quadcopter about the u_z axis and it can be obtained by having a difference in the torque developed by each pair of propellers. The torque can be changed by having a bigger angular speed on one of the propeller pairs over the other. Both negative and positive yaw motions can be seen in cases (e) and (f).

- **Translational motion** or vertical movement can be obtained by equally increasing or decreasing the angular speeds of all motors as seen in cases (g) and (h).

2.4 Assumptions

Given the fact that stabilizing a quadcopter is quite a complex problem, we will make a few general assumptions that will enable us to make a more simple version of the model:

- The quadcopter is symmetric along u_x and u_y .
- The quadcopter is a rigid body.
- The flapping effects of the rotors are ignored.
- Nonlinearities of the battery are ignored.
- Both accelerometer and gyroscope sensors are considered to be at the center of mass of the quadcopter.
- All motors have the same time constant.
- All aerodynamic forces acting on the quadcopter are ignored.

Chapter 3

Physical setup

This chapter will give a general overview on the pieces of technical equipment which we are using and show what the purpose of each one is. In addition, a diagram of the wiring of the components can be found in Appendix X.

Motors

Controlling a quadcopter can be done efficiently by using high-quality motors with fast response, which will ensure more of a stable flight. The motors must also be powerful enough to be able to lift the quadcopter and perform the required aerial movements.

The motor that we are using is the Turnigy Multistar Brushless Motor seen in Figure 3.1.



Figure 3.1: Turnigy Multistar 2213-980 V2 Brushless Motor.

Propellers

The propellers don't have such strict requirements as the motors. They are needed to be light and have a size and lift potential in order for the quadcopter to hover

at less than 50% of the motor capacity. For our quadcopter, we are using plastic 10x4.5" propellers with light weight - 60g. They have a length of 254 mm and a pitch inclination of 114mm. They can be seen in Figure 3.2.



Figure 3.2: Hobbyking Slowfly Propeller 10x4.5.

Electric Speed Controller

Electronic Speed Controller (ESC) is a widely used device in rotorcrafts. The purpose of an ESC is to vary the electric motor's speed. They also come with programmable features, such as braking or selecting appropriate type of battery. We need the ESC to have a fast response, for the same reasons mentioned for the motors in Section ???. The ESC that we are using is the TURNIGY Plush 30A which is shown in Figure 3.3.



Figure 3.3: TURNIGY Plush 30A Speed Controller.

APM Flight Controller

ArduPilotMega (APM) is an open source unmanned aerial vehicle (UAV) platform which is able to control autonomous multicopters. It is illustrated in Figure 3.4. The system was improved uses Inertial Measurement Unit (IMU) - a combination

of accelerometers, gyroscopes and magnetometers. The "Ardu" part of the project name shows that the programming can be done using Arduino open-source language.

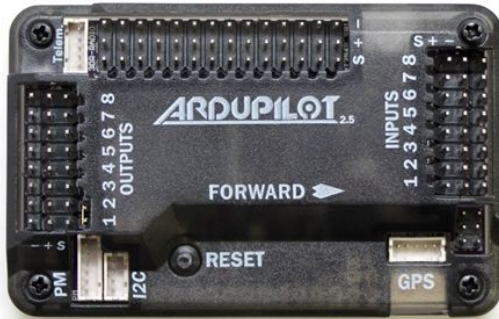


Figure 3.4: APM 2.5 board.

Power Distribution Board

To reduce the number of connections straight to the battery, we used the a power distribution board made for a previous project. A board like this is an easy solution since it enables us to connect the four ESCs directly to the board and then connect the board to the battery.

Battery

To power up our quadcopter, we will use a TURNIGY nano-tech Lipoly battery, which can be seen in Figure 3.5. Higher voltage under load, straighter discharge curves and excellent performance are the factors that make it suitable for our project.



Figure 3.5: Turnigy nano-tech 6000mah 3S 25 50C Lipo Pack.

Chapter 4

Quadcopter Model

Quadcopter control is a complex, yet interesting problem. One of the reasons why this control problem is challenging is the fact that a quadcopter has six degrees of freedom, but only four inputs which affects the linearity of the dynamics and makes the quadcopter underactuated.

In this chapter we will take a look at the kinematics and dynamics equations that describe our quadcopter system.

4.1 Quaternions and Euler angles

In Section , we have explained how the position of the quadcopter is expressed in the inertial frame and how the velocity of the quadcopter is express in the body-fixed frame. Therefore, we need to be able to find a relationship between the two, so that we can move from one to the other.

Euler angles have to be applied as a sequence of rotations. This report will use the *roll, pitch, yaw* convention. Therefore, the roll rotation will be $(R(\phi)^T)$, the pitch rotation will be $(R(\theta)^T)$ and the yaw rotation will be $(R(\psi)^T)$. Equations , and describe the quadcopter's orientation relative to the inertial frame in matrix form:

$$R(\phi)^T = \begin{bmatrix} 1 & 0 & 0 \\ 0 & \cos\phi & \sin\phi \\ 0 & -\sin\phi & \cos\phi \end{bmatrix} \quad (4.1)$$

$$R(\theta)^T = \begin{bmatrix} \cos\theta & 0 & -\sin\theta \\ 0 & 1 & 0 \\ \sin\theta & 0 & \cos\theta \end{bmatrix} \quad (4.2)$$

$$R(\psi)^T = \begin{bmatrix} \cos\psi & \sin\psi & 0 \\ -\sin\psi & \cos\psi & 0 \\ 0 & 0 & 1 \end{bmatrix} \quad (4.3)$$

Merging the three rotations as:

$$S = R(\phi)^T R(\theta)^T R(\psi)^T \quad (4.4)$$

gives the rotation matrix - S , which expresses a vector from the inertial frame to the body-fixed frame:

$$S = \begin{bmatrix} \cos\theta\cos\psi & \cos\theta\sin\psi & -\sin\theta \\ \cos\psi\sin\phi\sin\theta - \cos\phi\sin\psi & \sin\psi\sin\theta\sin\phi + \cos\phi\cos\psi & \cos\theta\sin\phi \\ \cos\psi\cos\phi\sin\theta & \cos\phi\sin\theta\sin\psi - \cos\psi\sin\phi & \cos\theta\cos\phi \end{bmatrix} \quad (4.5)$$

We can notice that if we were to have $\theta = \Pi/2$, the rotation matrix brings out a singularity by turning into:

$$S = \begin{bmatrix} 0 & 0 & -1 \\ \sin(\phi - \psi) & \cos(\phi - \psi) & 0 \\ \cos(\phi - \psi) & -\sin(\phi - \psi) & 0 \end{bmatrix} \quad (4.6)$$

As a result, one degree of freedom in the three dimensional space is lost. In addition, a change in either ϕ or ψ will now have the same effect, which causes confusion. In order to be able to avoid this problem, a quaternion-based method can be applied instead.

A quaternion can be expressed as $q = [q_0, q_1, q_2, q_3]^T$, which yields:

$$q = \begin{bmatrix} \cos(\phi/2)\cos(\theta/2)\cos(\psi/2) + \sin(\phi/2)\sin(\theta/2)\sin(\psi/2) \\ \sin(\phi/2)\cos(\theta/2)\cos(\psi/2) - \cos(\phi/2)\sin(\theta/2)\sin(\psi/2) \\ \cos(\phi/2)\sin(\theta/2)\cos(\psi/2) + \sin(\phi/2)\cos(\theta/2)\sin(\psi/2) \\ \cos(\phi/2)\cos(\theta/2)\sin(\psi/2) - \sin(\phi/2)\sin(\theta/2)\cos(\psi/2) \end{bmatrix} \quad (4.7)$$

The quaternion and Euler angles are equivalent in terms of attitude, therefore we can convert from one representation to the other. The rotation matrix can be then rewritten as:

$$S_q = \begin{bmatrix} 1 - 2(q_2^2 + q_3^2) & 2(q_1q_2 + q_3q_0) & 2(q_1q_3 - q_2q_0) \\ 2(q_1q_2 - q_3q_0) & 1 - 2(q_1^2 + q_3^2) & 2(q_2q_3 + q_1q_0) \\ 2(q_1q_3 + q_2q_0) & 2(q_2q_3 - q_1q_0) & 1 - 2(q_1^2 + q_2^2) \end{bmatrix} \quad (4.8)$$

4.2 BLDC Motor

The mathematical model of a BLDC motor is many ways similar to the one of a conventional DC motor. The main difference is represented by the added phases which affect the resistive and inductive components of the BLDC arrangement.

Therefore, we will start of by describing the mathematical modelling of a DC motor and then change it to fit the BLDC motor.

Figure illustrates a DC electromechanical system.

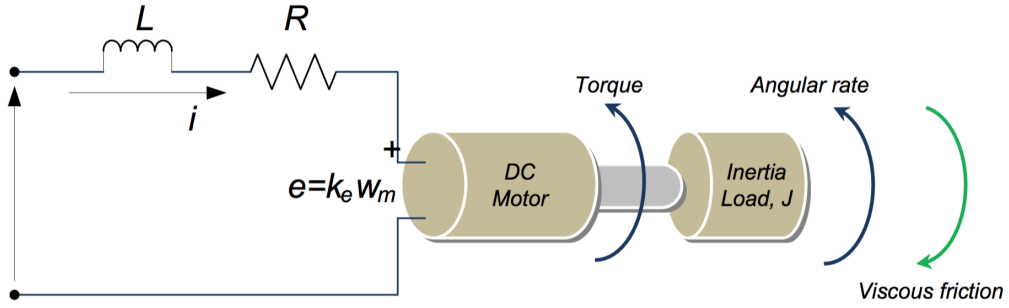


Figure 4.1: Typical DC electromechanical system

The components of the electrical circuit are the armature resistance - R, the armature inductance - L and the back EMF - e. By applying KVL, we obtain:

$$V_s = Ri + L \frac{di}{dt} + e \quad (4.9)$$

where V_s - DC source voltage and i - armature current.

Moving on to the mechanical part, further equations can be written using Newton's second law of motion:

$$J \frac{d\omega_m}{dt} = \sum T_i \quad (4.10)$$

$$T_e = k_f + J \frac{d\omega_m}{dt} + T_L \quad (4.11)$$

where T_e - electrical torque, k_f - friction constant, J - rotor inertia, ω_m - angular velocity and T_L - load torque.

The back EMF and the electrical torque can be described as:

$$T_e = k_t \omega_m \quad (4.12)$$

$$e = k_e \omega_m \quad (4.13)$$

where k_e - back EMF constant and k_t - torque constant.

Rewriting equations 4.9 and 4.10 gives:

$$\frac{di}{dt} = -i \frac{R}{L} - \frac{k_e}{L} \omega_m + \frac{1}{L} V_s \quad (4.14)$$

$$\frac{d\omega_m}{dt} = i \frac{k_t}{J} - \frac{k_f}{J} \omega_m + \frac{1}{J} T_L \quad (4.15)$$

Taking the Laplace transform of 4.14 and 4.15 yields:

$$si = i \frac{R}{L} - \frac{k_e}{L} \omega_m + \frac{1}{L} V_s \quad (4.16)$$

$$s\omega_m = i \frac{k_t}{J} - \frac{k_f}{J} \omega_m + \frac{1}{J} T_L \quad (4.17)$$

The next equation is obtained by substituting i from equation 4.17 into 4.16.

$$\left(\frac{s\omega_m + \frac{k_f}{J} \omega_m - \frac{1}{J} T_L}{\frac{k_t}{J}} \right) \left(s + \frac{R}{L} \right) = -\frac{k_e}{L} \omega_m + \frac{1}{L} V_s \quad (4.18)$$

Assuming there is no load, equation 4.18 can be rewritten as:

$$\left\{ \left(\frac{s^2 J}{k_t} + \frac{sk_f}{k_t} + \frac{sRJ}{k_t L} + \frac{k_f R}{k_t L} \right) + \frac{k_e}{L} \right\} \omega_m = \frac{1}{L} V_s \quad (4.19)$$

Solving 4.19 gives:

$$V_s = \frac{s^2 JL + sk_f L + sRJ + k_f R + k_e k_t}{k_t} \omega_m \quad (4.20)$$

The transfer function can be obtained as the ratio between the angular velocity ω_m and the source voltage V_s :

$$G_s = \frac{\omega_m}{V_s} = \frac{k_t}{s^2 JL + (RJ + k_f L)s + k_f R + k_e k_t} \quad (4.21)$$

Considering that k_f tends to zero, the transssfer function can finally be written as:

$$G_s = \frac{\omega_m}{V_s} = \frac{k_t}{s^2 JL + RJs + k_e k_t} \quad (4.22)$$

In order to obtain the mechanical and electrical time constants, we will need to manipulate equation 4.22, which gives:

$$G_s = \frac{\frac{1}{k_e}}{\frac{RJ}{k_e k_t} \frac{L}{R} s^2 + \frac{RJ}{k_e k_t} s + 1} \quad (4.23)$$

where the mechanical time constant is:

$$\tau_m = \frac{RJ}{k_e k_t} \quad (4.24)$$

and the electrical time constant is:

$$\tau_e = \frac{L}{R} \quad (4.25)$$

Therefore, substituting equations 4.24 and 4.25 into equation 4.23 yields:

$$G_s = \frac{\frac{1}{k_e}}{\tau_m \tau_e s^2 + \tau_m s + 1} \quad (4.26)$$

Equations 4.23 - 4.25 will now be changed in order to fit a BLDC motor. Therefore, they will become:

$$\tau_m = \Sigma \frac{RJ}{k_e k_t} = \frac{J \Sigma R}{k_e k_t} \quad (4.27)$$

$$\tau_e = \Sigma \frac{L}{R} = \frac{L}{\Sigma R} \quad (4.28)$$

Having a symmetrical arrangement and a three phase motor, the constants will finally be:

$$\tau_m = \frac{J3R}{k_e k_t} \quad (4.29)$$

$$\tau_e = \frac{L}{3R} \quad (4.30)$$

Taking into account the phase effects, τ_m will be rewritten as:

$$\tau_m = \frac{J3R_\phi}{k_e k_t} \quad (4.31)$$

with k_e now being the phase value of the back EMF voltage time constant described by:

$$k_e = k_{e(L-L)} / \sqrt{3} \quad (4.32)$$

A relationship between k_e - electrical torque and k_t - torque constant is found in equation 4.33 by using the electrical power and mechanical power formulas.

$$k_e = k_t \times 0.0605 \quad (4.33)$$

The next step in coming up with a final transfer function for our motor is to find τ_m and τ_e , which are functions of k_e , k_t , R_ϕ , J and L .

A numerical value for k_e can be obtained using equation 4.32:

$$k_e = \frac{11.1}{1.73} = 6.416 \quad (4.34)$$

Since k_t is a function of k_e , its numerical value can also be found using equation 4.33:

$$k_t = \frac{6.416}{0.0605} = 106.04 \quad (4.35)$$

For R_ϕ , we have to measure the line-to-line resistance (between any two wires of the motor) and divide the result by 2 in order to get its value.

experiments on J and L / take them from other reports

4.3 Quadcopter Dynamics

To start describing drone's dynamics, we illustrate two frames - the inertial frame, which is defined by the ground, where the negative z direction shows represents gravity and the body frame. In the body frame, the motor axes point in the positive z direction and the arms point in the x and y directions. These two frames can be seen in figure 4.2.

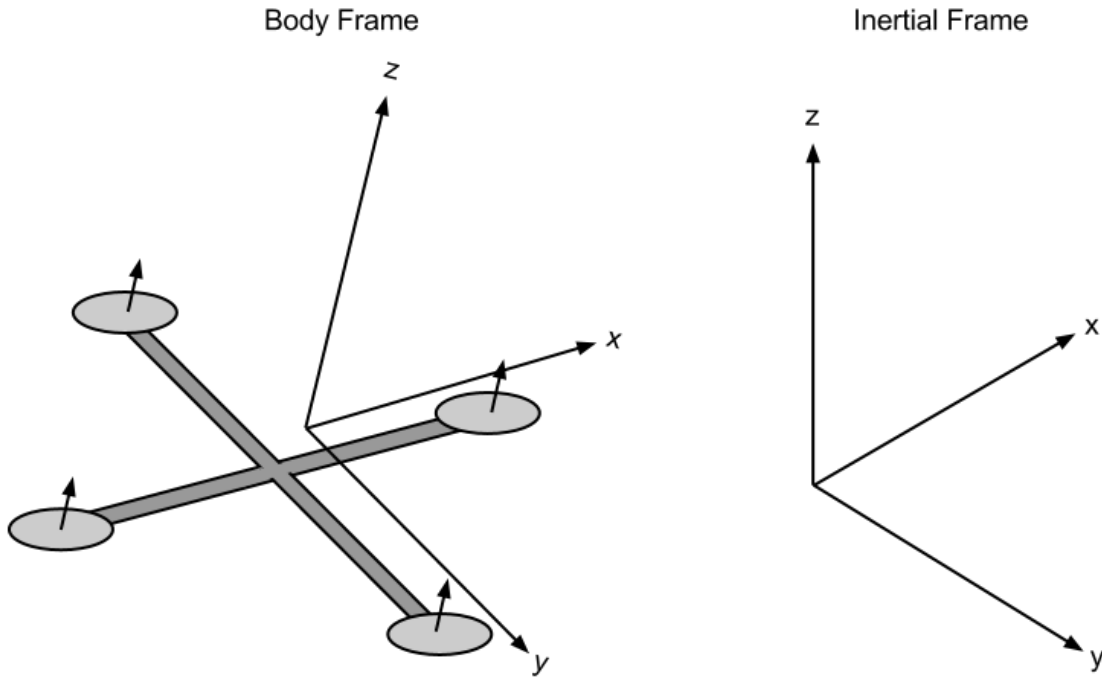


Figure 4.2: Quadcopter Body Frame and Inertial Frame

4.4 Kinematics

The drone's position in inertial frame is defined as $x = (x, y, z)^T$. Similarly, the velocity is $\dot{x} = (\dot{x}, \dot{y}, \dot{z})^T$. In the body frame, we have the roll, pitch and yaw angles given to be $\theta = (\phi, \theta, \Psi)^T$. Then, the angular velocities are equal to $\dot{\theta} = (\dot{\phi}, \dot{\theta}, \dot{\psi})^T$. It should be noted that the angular velocity vector ω is not equal to the angular velocity $\dot{\theta}$ itself. It is possible to convert angular velocity into angular velocity vector using the following expression:

$$\omega = \begin{bmatrix} 1 & 0 & -s_\theta \\ 0 & c_\phi & c_\theta s_\phi \\ 0 & -s_\phi & c_\theta c_\phi \end{bmatrix} \dot{\theta} \quad (4.36)$$

where ω is the angular velocity vector.

Both frames can be related using a rotation matrix R , which goes from one frame to another. The matrix is obtained using the ZYZ Euler angle conventions.

$$R = \begin{bmatrix} c_\phi c_\psi - c_\theta s_\phi s_\psi & -c_\psi s_\phi - c_\phi c_\theta s_\psi & s_\theta s_\psi \\ c_\theta c_\psi s_\phi + c_\phi s_\psi & c_\phi c_\theta c_\psi - s_\phi s_\psi & -c_\psi s_\theta \\ s_\phi s_\theta & c_\phi s_\theta & c_\theta \end{bmatrix} \quad (4.37)$$

Therefore, a vector \vec{v} in the body frame can be defined as $R\vec{v}$ in the inertial frame.

4.5 Motor Dynamics

A brushless motor produces torque given by equation 4.38.

$$\tau = K_t(I - I_0) \quad (4.38)$$

Here, τ is the torque, I is the input current, K_t is the constant describing torque proportionality and I_0 is the no-load current.

The voltage on the motor is the sum of a resistive loss and the Back-EMF, giving equation 4.39.

$$V = IR_m + K_e\omega \quad (4.39)$$

where V is the voltage across the motor, R_m is the motor resistance, ω is the angular velocity and K_e is a constant, describing the back-EMF generated per RPM. We can then combine equations 4.38 and 4.39 and put them into the power equation, to get a new equation 4.40.

$$P = IV = \frac{(\tau + K_t I_0)(K_t I_0 R_m + \tau R_m + K_t K_e \omega)}{K_t^2} \quad (4.40)$$

To help simplify the model, we can assume that the motor resistance is very small and therefore can be disregarded. This gives us a new power equation 4.41.

$$P \approx \frac{(\tau + K_t I_0)K_e\omega}{K_t} \quad (4.41)$$

We can also, for the purposes of simplifying the model, assume that $K_t I_0 \ll \tau$. This is a reasonable assumption due to the fact that I_0 describes the current with no load on the motor and is usually a small number. Based on this, we can then obtain the final equation 4.42 for power.

$$P \approx \frac{K_e}{K_t} \tau \omega \quad (4.42)$$

4.6 Forces

From the conservation of energy, it is known that the energy that the motor expends during some period of time is equal to the force generated by the propeller multiplied by the distance the it displaces moves, given by the equation 4.43.

$$P \times dt = F \times dx \quad (4.43)$$

We can then say that the power is also equal to the thrust multiplied by the air velocity, as seen in equation 4.44.

$$P = F \frac{dt}{dx} = T v_h \quad (4.44)$$

Here - T is the thrust and v_h is the air velocity. Since the model is describing a hovering quadcopter in a closed area, only v_h is an acting velocity (i.e. vehicle speed has no effect and free stream velocity is equal to zero).

Momentum theory gives equation 4.45, for the hover velocity v_h .

$$v_h = \sqrt{\frac{T}{2\rho A}} \quad (4.45)$$

where A is the area swept out by the blade and ρ is the air density. In the case of this model, τ is proportional to thrust T by a constant K_τ . Keeping this in mind, we can now use the simplified power equation 4.42 and derive a new equation 4.46.

$$P = \frac{K_e}{K_t} \tau \omega = \frac{K_e K_\tau}{K_t} T \omega = \frac{F^{\frac{3}{2}}}{\sqrt{2\rho A}} \quad (4.46)$$

Solving for thrust T , we can derive a new equation 4.47.

$$T = \left(\frac{K_e K_\tau \sqrt{2\rho A}}{K_t} \omega \right)^2 = k \omega^2 \quad (4.47)$$

where k is a constant, describing all other constants used in the equation.

The final equation 4.47 now describes the thrust T generated by the motor with angular velocity ω as an input.

We can now sum the thrust over all motors. This sum is then given by

$$T_B = \sum_{i=1}^4 T_i = k \begin{bmatrix} 0 \\ 0 \\ \sum \omega_i^2 \end{bmatrix} \quad (4.48)$$

We can model a simplified version of fluid friction as a force proportional to the linear velocity in each direction. Then, drag forces will have another force term in their model:

$$\mathbf{F}_D = \begin{bmatrix} -k_d \dot{x} \\ -k_d \dot{y} \\ -k_d \dot{z} \end{bmatrix} \quad (4.49)$$

4.7 Torques

Every motor produces some torque about the z axis in the body frame. This torque is the requirement for the torque produced by the motor to keep the motor providing thrust by spinning the propeller. The spinning propeller overcomes frictional forces and creates angular acceleration. The frictional force is acquired from fluid dynamics as follows:

$$F_D = \frac{1}{2} \rho C_D A v^2 \quad (4.50)$$

Here, ρ is the fluid density, A is the propeller cross-section area, C_D is a dimensionless constant. We can then derive an equation for torque produced due to drag force:

$$\tau_D = \frac{1}{2} R \rho C_D A v^2 = \frac{1}{2} R \rho C_D A (\omega R)^2 = b \omega^2 \quad (4.51)$$

where b is an appropriately dimensioned constant. While we assume that force all of the force is applied at the top of the propeller, our only concern is that the drag torque is proportional to the angular velocity. Torque for the i^{th} motor about the z axis can then be described as follows:

$$\tau_z = (-1)^{i+1} b \omega^2 + I_M \dot{\omega} \quad (4.52)$$

Here, I_M is the moment of inertia about the z axis of the motor, $\dot{\omega}$ is the angular acceleration of the propeller and the term $(-1)^{i+1}$ is describing the direction of rotation of the i^{th} motor (i.e. whether it is spinning clockwise or counter-clockwise). Since in a steady state there is no acceleration, we can say that $\dot{\omega} \approx 0$ and drop the term. The simplified equation then becomes

$$\tau_z = (-1)^{i+1} b \omega^2 \quad (4.53)$$

Then, we can derive an equation for total torque about the z axis.

$$\tau_\psi = b(\omega_1^2 - \omega_2^2 + \omega_3^2 - \omega_4^2) \quad (4.54)$$

If we select motors 1 and 3 to be on the roll axis, we can the following roll torque equation:

$$\tau_\phi = \sum r \times T = L(k\omega_1^2 - k\omega_3^2) = Lk(\omega_1^2 - \omega_3^2) \quad (4.55)$$

Here, L defines the distance from the propeller to the centre of the quadcopter, assuming all motors are placed at equal distances. Similarly, we can obtain the pitch torque for the other two motors:

$$\tau_\theta = Lk(\omega_2^2 - \omega_4^2) \quad (4.56)$$

A matrix describing all torques in the body frame can be seen in equation 4.57.

$$\tau_B = \begin{bmatrix} Lk(\omega_1^2 - \omega_3^2) \\ Lk(\omega_2^2 - \omega_4^2) \\ b(\omega_1^2 - \omega_2^2 + \omega_3^2 - \omega_4^2) \end{bmatrix} \quad (4.57)$$

4.8 Equations of Motion

Quadcopter's acceleration in the inertial frame is caused by gravity, thrust and linear force. We can obtain thrust vector in the inertial frame through the use of rotation matrix R to map thrust vector from one frame to the other. Linear motion can then be described by equation 4.58.

$$m\ddot{x} = \begin{bmatrix} 0 \\ 0 \\ -mg \end{bmatrix} \quad (4.58)$$

Since we prefer to express rotations about the centre of the vehicle instead of about inertial centre, it is more reasonable to use rotational equations of motion in body frame. We can derive these equations from Euler's equations for rigid body dynamics. The equation 4.59 is expressed in vector form.

$$I\dot{\omega} + \omega \times (I\omega) = \tau \quad (4.59)$$

It can then be rewritten as equation 4.60.

$$\dot{\omega} = \begin{bmatrix} \dot{\omega}_x \\ \dot{\omega}_y \\ \dot{\omega}_z \end{bmatrix} = I^{-1}(\tau - \omega \times (I\omega)) \quad (4.60)$$

A drone model can be understood as two lines crossed together at origin with a point mass as motors at the end of each line. From this, we can derive a diagonal inertia matrix 4.61.

$$I = \begin{bmatrix} I_{xx} & 0 & 0 \\ 0 & I_{yy} & 0 \\ 0 & 0 & I_{zz} \end{bmatrix} = I^{-1}(\tau - \omega \times (I\omega)) \quad (4.61)$$

Taking everything into consideration, a final result for the rotational equations of motion in body frame are given as equation 4.62.

$$\dot{\omega} = \begin{bmatrix} \tau_\phi I_{xx}^{-1} \\ \tau_\theta I_{yy}^{-1} \\ \tau_\psi I_{zz}^{-1} \end{bmatrix} - \begin{bmatrix} \frac{I_{yy}-I_{zz}}{I_{xx}}\omega_y\omega_z \\ \frac{I_{zz}-I_{xx}}{I_{yy}}\omega_x\omega_z \\ \frac{I_{xx}-I_{yy}}{I_{zz}}\omega_x\omega_y \end{bmatrix} \quad (4.62)$$

4.9 Control

Having a mathematical model of the system makes the development of controller easier. With only input being the angular velocities of each motor, we can write the system as a first order differential equation in state space.

$$\dot{x}_1 = x_2 \quad (4.63)$$

$$\dot{x}_2 = \begin{bmatrix} 0 \\ 0 \\ -g \end{bmatrix} + \frac{1}{m} RT_B + \frac{1}{m} F_D \quad (4.64)$$

$$\dot{x}_3 = \begin{bmatrix} 1 & 0 & -s_\theta \\ 0 & c_\phi & c_\theta s_\phi \\ 0 & -s_\phi & c_\theta c_\phi \end{bmatrix}^{-1} x_4 \quad (4.65)$$

$$\dot{x}_4 = \begin{bmatrix} \tau_\phi I_{xx}^{-1} \\ \tau_\theta I_{yy}^{-1} \\ \tau_\psi I_{zz}^{-1} \end{bmatrix} - \begin{bmatrix} \frac{I_{yy}-I_{zz}}{I_{xx}} \omega_y \omega_z \\ \frac{I_{zz}-I_{xx}}{I_{yy}} \omega_x \omega_z \\ \frac{I_{xx}-I_{yy}}{I_{zz}} \omega_x \omega_y \end{bmatrix} \quad (4.66)$$

Here, x_1 is the position of the vehicle in space, x_2 is the drone's linear velocity, x_3 denotes the angles of pitch, roll and yaw and x_4 shows the angular velocity vector.

Chapter 5

Sensors

...

5.1 Model of the sensors

Accelerometer

Gyroscope

5.1.1 Programming Accelerometer and Gyroscope

The accelerometer and gyroscope that we are using are both part of the built-in IMU of the Ardupilot and they are 3-axis. The accelerometer works by detecting a force that is actually the opposite of the acceleration vector. This force is not always caused by acceleration, but it can be. It just happens that acceleration causes an inertial force that is captured by the force detection mechanism of the accelerometer. The gyroscope measures the rotation around one of the axes.

It is important to understand how the sensors can actually deliver us the data. Usually, they fall into two categories: analog and digital. The one we are using is digital and it can be programmed using I2C, SPI or USART communication.

//insert lines of code that makes the spi communication possible

Before getting into the calculations of the angles, we need to get the raw values from both accelerometer and gyroscope and that is done by accessing their registers.

//insert lines of code that read the raw values from acc and gyro

If we want to calculate the inclination of a device relative to the ground for example, we can calculate the angle between the force vector and one of the z-axis. We can do that by manipulating the raw values and by degree conversion. The functions

that take care of converting the raw values from both accelerometer and gyroscope are the following:

//insert lines of code for the math part

We have used the Serial Monitor within the Arduino IDE environment to read the outputs from both sensors and they seem to be accurate. The difference in the values of the acceleromter output is because accelerometers are more sensitive to noise and vibrations. The figure below shows the printed outputs at steady state, that is when the quadcopter is parallel to the ground.

//insert printscrean of the values

//mention sensitivity

Chapter 6

Actuators

-intro-

6.1 Propeller model

...

6.2 Motor model

Andy

6.2.1 Expected and Real Motor Performance

The motors used in the prototype specify to be rated at K_v of 980. K_v is a constant describing the ratio between RPM and the applied voltage and is expressed as $K_v = \frac{RPM}{V}$. Derived from this, voltage's effect on the RPM can be seen in figure 6.1.

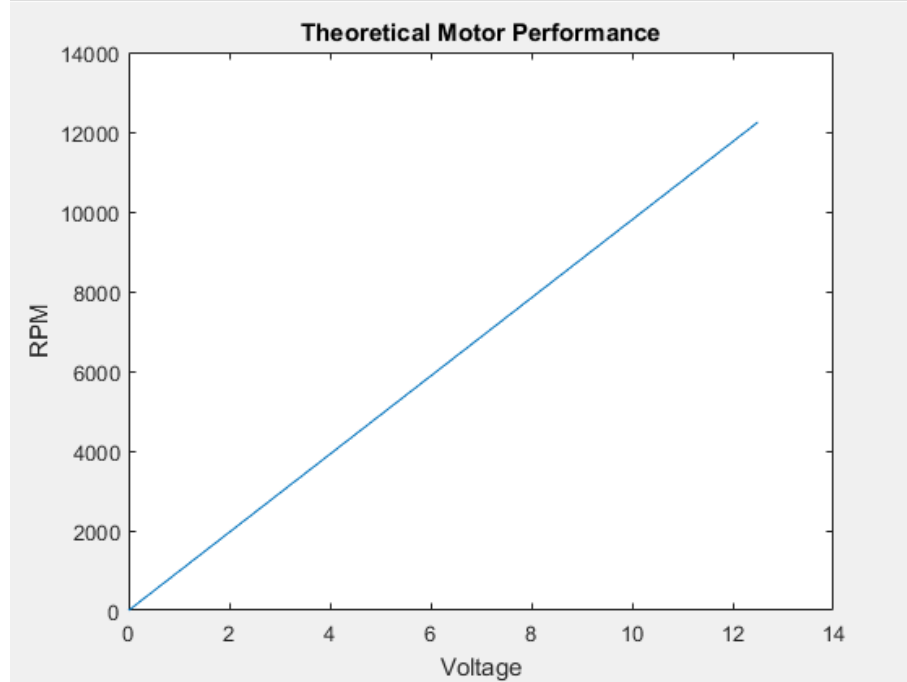


Figure 6.1: Expected motor performance

With a fully charged battery, the RPM is expected to be $980 \times 11.1V = 10878RPM$.

In order to confirm this, the actual RPM was measured using SHIMPO DT-205 digital tachometer. A piece of reflective paper was taped to one of the motors so that the tachometer would have something to lock onto, as seen in figure 6.2.

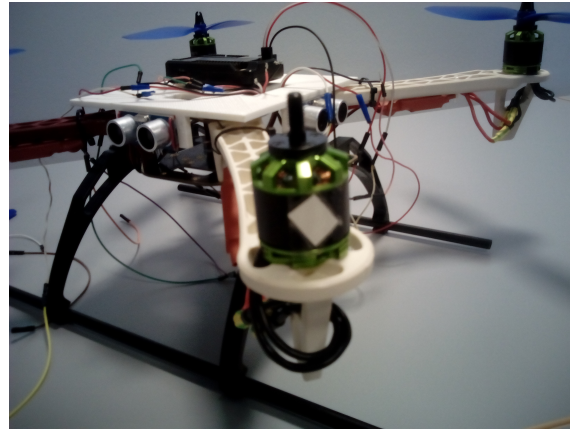


Figure 6.2: Reflective paper on the motor

By sending the maximum signal from the board, the RPM was measured to be 10812, with a small possible error. In conclusion, the motors' K_v coefficient found in the datasheet is in fact correct.

6.2.2 APM Output and Motor Speed Relationship

In order to use the board's output signal as an input in a mathematical model, it is necessary to find an equation to translate it into an angular rate. First, an equation has been found that describes the relationship between motor's RPM, ESC's output signal frequency and number of motor poles [3]:

$$RPM = \frac{120 \times f}{n} \quad (6.1)$$

Here, f is the frequency and n is the number of poles (in the case of this project - 14).

Therefore, it is possible to measure the frequency at various output values, which can then be used to define an equation that uses the board's signal length as an input value and results in an RPM.

The frequency was measured using an (NAME) oscilloscope and by connecting the probe's ground clip to the ground of the battery and the probe tip to any one of the wires between motor and the ESC. Then, by providing different output signals from the flight controller, the frequency was measured on the oscilloscope screen. An on-board filter was used to filter out some noise, especially at lower output signals. The recorded frequency was later converted into RPM using equation 6.1, for later comparison. The output signal lengths and the corresponding frequencies converted into RPM can be seen in table 6.1.

<i>Output, μs</i>	<i>RPM</i>
762	2825
770	3189
780	3689
790	4211
800	4683
810	5161
820	5546
830	5874
840	6223
850	6532
860	6795
870	7008
880	7301
890	7534
900	7730
925	8233
950	8552
975	8786
1000	9129
1050	9566
1100	9814
1150	10071
1200	10260

Table 6.1: Frequency measured at ESC output, converted into RPM

While measuring, it was observed that the frequency would never reach a steady-state and therefore, a sizeable error is possible between measurements. Because of that, RPM was manually measured using the tachometer at same output values, as seen in table 6.2.

<i>Output, μs</i>	<i>RPM</i>
762	2754
770	3170
780	3664
790	4210
800	4715
810	5223
820	5617
830	5965
840	6285
850	6578
860	6846
870	7100
880	7368
890	7555
900	7790
925	8265
950	8614
975	8910
1000	9160
1050	9576
1100	9860
1150	10089
1200	10261

Table 6.2: RPM measured at different values

While measuring with tachometer, the error appeared to be less significant.

The two tables 6.2 and 6.1 were then plotted to see the difference, which is seen in figure 6.3.

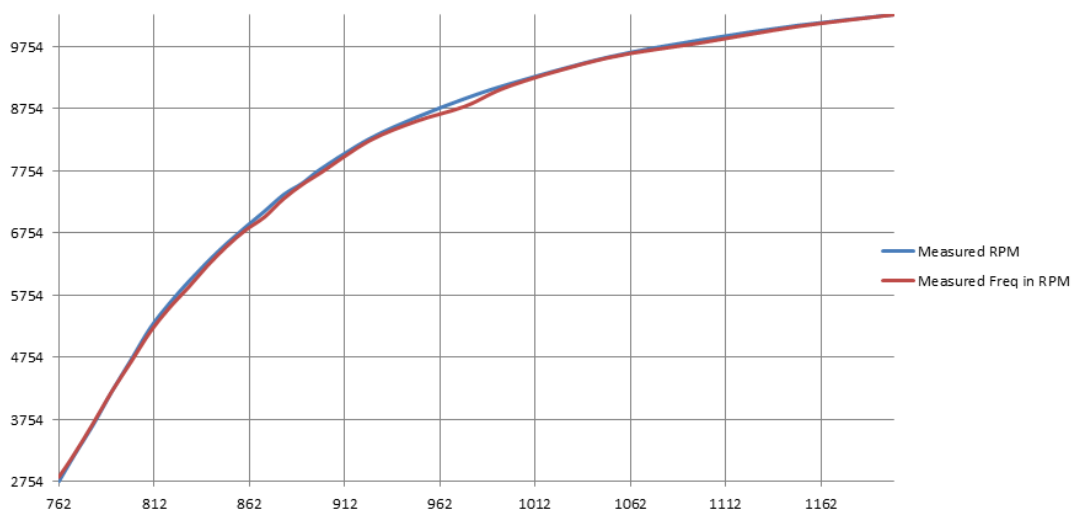


Figure 6.3: Plotted values of manually measured and frequency-based RPM

From the plotted graphs, it can be seen that the difference is very much noticeable, especially at certain points. Due to the fact that measurements with tachometer provided smaller errors than measurements with an oscilloscope, it was decided to use the values measured with the tachometer for later calculations.

In order to make use of these findings, the RPM values have to be converted into *rad/s* for use as angular rate. The conversion equation is:

$$\omega = \frac{2\pi \times RPM}{60} \quad (6.2)$$

The values measured with tachometer were then converted into *rad/s* and plotted on a Microsoft Excel 2010. Then, by utilising the "Format Trendline" function, a 4th order polynomial equation fitting the original graph was obtained. The values and graphs can be seen in figure 6.4.

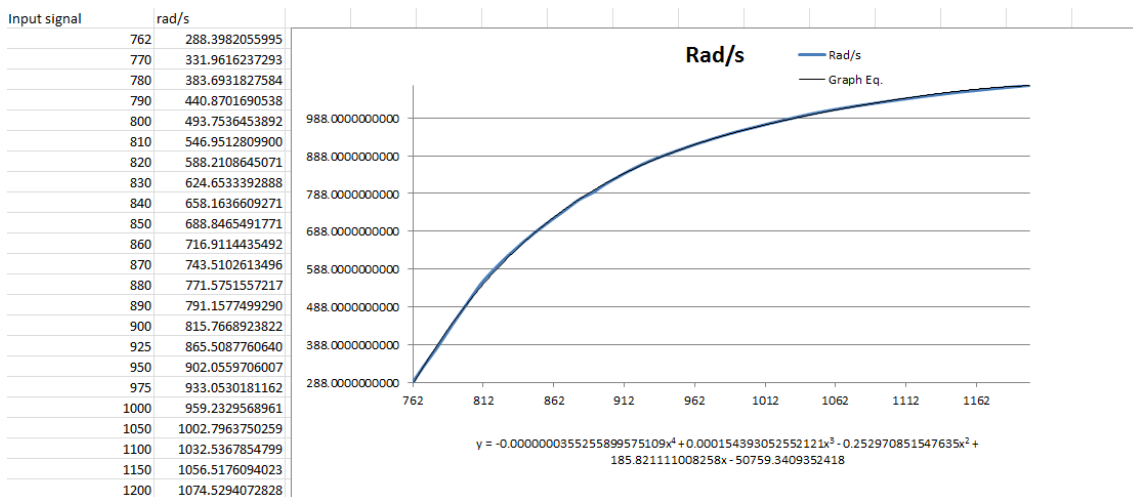


Figure 6.4: Converted and plotted RPM values and the trendline

This equation, $y = -0.0000000355255899575109x^4 + 0.000154393052552121x^3 - 0.252970851547635x^2 + 185.821111008258x - 50759.3409352418$, can then be used to approximately convert the signal sent out by the flight controller in μs into angular rate.

6.3 Electronic Speed Controllers

...

6.3.1 Calibrating and Programming ESCs

ESCs have 5 input pins, 3 of which come from the flight controller. These 3 wires supply the signal for the ESC to translate into the angle of the shaft for the motor. Before ESCs can be used, they need to be properly calibrated. Programming additional settings is optional, but in most cases necessary too. Normally, the calibration for UAVs is done by setting the throttle to full on the radio controller before powering the ESCs. However, since the board translates the throttle signal into a PWM signal, it is possible to calibrate and run the motors directly from the flight controller by sending a PWM signal using software.

The calibration is done by first sending the maximum length of signal the user wishes to use. The ESC emits sounds that are brand-specific and indicate whether the signal was successfully recognised or not. Once the maximum signal is accepted, the user emits the minimum signal and waits for approval. Additional sound is then emitted, indicating that the calibration was successful.

Using Arduino's Servo library, a self-explanatory built-in function `servo.writeMicroseconds(int value)` is used to send the signal. By default, the library has the minimum signal set to $544\mu s$ and the maximum - to $2400\mu s$. For this project, we shortened the range down to $700\mu s$ and $2000\mu s$ for both signals respectively. A commented code used to calibrate the ESC connected to the first pin of the board can be seen in listing 6.1.

```

1 #define MAX_SIGNAL 2000 //define max and min signal length
2 #define MIN_SIGNAL 700
3 #define MOTOR_PIN1 12 //pin 1 on the board
4 Servo motor1;
5 void setup() {
6     Serial.begin(9600); //begin serial communication at 9600 rate
7     Serial.println("Program begin... ");
8     motor1.attach(MOTOR_PIN1); //attach the pin to the servo variable
9     Serial.println("Now writing maximum output.");
10    Serial.println("Turn on power source, then wait 2 seconds and press
11        any key.");
12    motor1.writeMicroseconds(MAX_SIGNAL); //this signal should only be
13        sent when calibrating for the first time
14    while (!Serial.available()); //wait for an input, so you have time to
15        plug in the ESC

```

```
13 Serial.read();
14 Serial.println("Sending minimum output");
15 motor1.writeMicroseconds(MIN_SIGNAL); //send the min signal, which is
16     the only needed signal when already calibrated
17 while (!Serial.available()); //wait for the beeps to indicate
18     calibration is done
19 Serial.read();
20 Serial.println("Calibrated");
21 }
22 void loop() {
23 }
```

Code Listing 6.1: Calibrating the ESC

Programming additional settings of the ESC is done in a similar manner - by sending minimum and maximum signals after the ESC emits particular sounds, indicating wanted selections. The programmable features and selections are brand-specific and can be found in the datasheets. For the purposes of this project, the ESCs have been programmed to include two features - brake mode off and selection of li-ion battery.

Chapter 7

State space model

Chapter 8

Experiments

8.0.1 Output Operating Range

Since there is no direct translation between the output signal from the board and the speed of the motor and the ESC allows more current than the motor can recognise, it is necessary to find the operating range for the board output that has the most noticeable effect on the RPM of the motor. Through trial and error and by measuring the RPM using SHIMPO DT-205 digital tachometer. The lowest operating point was found to be $762\mu s$, at which the motor finally begins to spin. The highest point was defined at $1200\mu s$. Higher values were found to have very small effect on the RPM. Therefore, despite the ESC recognising the values between 700 and $2000\mu s$, the most noticeable effect will be between 762 and $1200\mu s$ and will be primarily used in the project.

8.0.2 APM Frequency

Due to lack of proper documentation, it was necessary to do measure the frequency of the signals sent out by the flight controller. To do so, an oscilloscope was connected to one of the output pins of the board. Then, using the servo library, a signal was sent out. The interval between signals was found to be $20ms$, therefore, the frequency of the board is $50Hz$, as seen in figure 8.1.

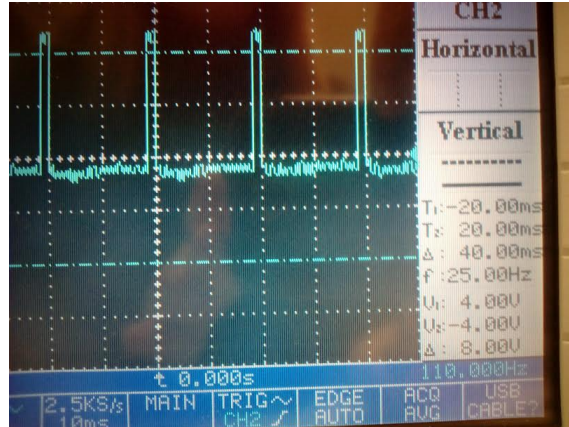


Figure 8.1: Oscilloscope measuring APM's frequency.

The second experiment on the board was then made to determine how the flight controller handles the output signals during those $20ms$. First two outputs of the APM were connected to the oscilloscope, both utilizing the Servo library to send signals of length of $2000\mu s$. Results can be seen in figure 8.2.

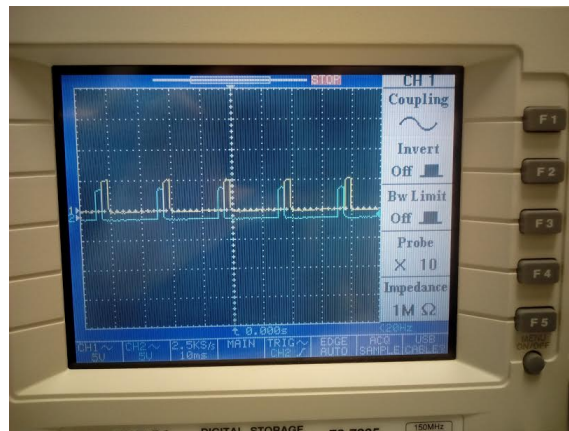


Figure 8.2: Readings of the two output signals.

Then, for further testing purposes, both outputs were given different values in two scenarios, as seen in figure 8.3.

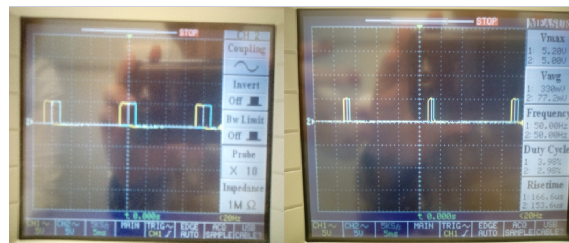


Figure 8.3: Left - signals running at $2000\mu s$; Right - $700\mu s$.

From this, two conclusions can be made:

1. If the first signal is shorter than the second one, the second signal will still follow right after the first signal ends. In other words, the APM leaves no gaps between the outputs.
2. Since the board runs at the frequency of $50Hz$ and has a period of $20ms$, this leaves $\frac{20}{8} = 2.5ms$ maximum length for each output signal. The servo library is hard-capped at $2.4ms$ and thus is well within the limits of the board.

Chapter 9

Discussion

Chapter 10

Conclusion

Bibliography

- [1] Nancy Hall. Simplified airplane motion. <https://www.grc.nasa.gov/www/k-12/airplane/smotion.html>. (Accessed 06/11/16).
- [2] Alex. The quadcopter : control the orientation. <http://theboredengineers.com/2012/05/the-quadcopter-basics/>. (Accessed 06/11/16).
- [3] Vfds how do i calculate rpm for three phase induction motors? <http://www.precision-elec.com/faq-vfd-how-do-i-calculate-rpm-for-three-phase-induction-motors/>. (Accessed 19/11/16).

Chapter 11

Appendix

11.1 Appendix code